Automatica 108 (2019) 108495

Contents lists available at ScienceDirect

Automatica

journal homepage: www.elsevier.com/locate/automatica

Brief paper

Curvature-constrained path elongation with expected length for Dubins vehicle[☆]

Yulong Ding[a], Bin Xin[a,b,c,*], Jie Chen[a,b,c]

[a] School of Automation, Beijing Institute of Technology, Beijing 100081, China
[b] Key Laboratory of Intelligent Control and Decision of Complex Systems, Beijing Institute of Technology, Beijing 100081, China
[c] Beijing Advanced Innovation Center for Intelligent Robots and Systems, Beijing 100081, China

ARTICLE INFO

Article history:
Received 11 February 2018
Received in revised form 3 March 2019
Accepted 28 June 2019
Available online 24 July 2019

Keywords:
Path elongation
Dubins vehicle
Terminal heading relaxation
Path planning
Maximum curvature constraint

ABSTRACT

Path elongation is a basic means of adjusting the time for a curvature-constrained vehicle to reach its destination, which is very common in the maneuvering control of high-speed vehicles or the coordinated control of their fleet. This paper studies the path elongation problem of a Dubins vehicle which moves in a two-dimensional plane and is subject to a maximum curvature. The aim of the paper is to answer the following question arising from the path elongation of Dubins vehicles: Can a Dubins vehicle reach a given destination by path elongation with a predefined path length? It is discovered and proved by theoretical analysis that, when the destination point is located in a special region, there is a special length interval for which no proper path exists. For all realizable length intervals, we provide an example of feasible path patterns for expected elongation. The results provide ideal reference trajectories with expected length for Dubins vehicles to follow for the sake of accurate arrival-time control.

1. Introduction

In the arrival-time control of autonomous vehicles, path elongation is a very common, feasible and safe means of adjusting the time to reach their destination, especially for meeting the requirement of maneuvering control of high-speed vehicles or the synchronization of arrival time of multiple cooperative vehicles. In this paper, we are concerned with the following fundamental problem about the path elongation of Dubins vehicle (Dubins, 1957):

Given an initial configuration and an endpoint, can a Dubins vehicle with curvature constraints in a two-dimensional plane move from its initial configuration to a specified endpoint with an expected path length?

The Dubins vehicle, with its position $(x, y) \in \mathbb{R}^2$, its heading θ and control input $u(|u| \leq 1)$, can be modeled by the following differential equation:

$$\begin{pmatrix} \dot{x} \\ \dot{y} \\ \dot{\theta} \end{pmatrix} = \begin{pmatrix} v_d \cos\theta \\ v_d \sin\theta \\ \frac{v_d u}{r_{\min}} \end{pmatrix} \tag{1}$$

where v_d and $r_{\min}$ are the speed and the minimum turning radius of the Dubins vehicle, respectively. Assume that v_d is a constant in the model. $\boldsymbol{\omega} = (x, y, \theta) \in SE(2)$ is called as Dubins configuration (Bui & Boissonnat, 1994; Dubins, 1957). There is a nonholonomic constraint in the Dubins model, that is $-\dot{x}\sin\theta + \dot{y}\cos\theta = 0$, which means that the Dubins vehicle must move in the direction of θ at each point. Dubins model has been successfully applied in different domains, such as terrestrial, aerial and underwater vehicles (Babel, 2017; Cao, Cao, Zeng, & Lian, 2016; Hernàndez, Moll, Vidal, Carreras, & Kavraki, 2016).

The shortest Dubins path can help the vehicle to save time and energy, and is often used to solve the Dubins traveling salesman problem (Zhang, Chen, Xin, & Peng, 2014). However, in order to satisfy the mission requirement (e.g., rendezvous Cao, Cao, Zeng, Yao, & Lian, 2017 and surveillance Zhang et al., 2014), the vehicle needs to timely arrive at its endpoint according to the given time or the expected path length. Constrained by the constant speed and the bounded curvature, the path length control method is of

☆ This work was supported in part by the National Outstanding Youth Talents Support Program, China 61822304, in part by the National Natural Science Foundation of China under Grant 61673058, in part by the NSFC-Zhejiang Joint Fund, China for the Integration of Industrialization and Informatization under Grant U1609214, in part by the Foundation for Innovative Research Groups of the National Natural Science Foundation of China under Grant 61621063, in part by the Projects of Major International (Regional) Joint Research Program of NSFC under Grant 61720106011 and in part by International Graduate Exchange Program of Beijing Institute of Technology, China. The material in this paper was not presented at any conference. This paper was recommended for publication in revised form by Associate Editor Zhihua Qu under the direction of Editor Daniel Liberzon.

* Corresponding author at: School of Automation, Beijing Institute of Technology, Beijing, 100081, China.

E-mail addresses: dingyvlong@bit.edu.cn (Y. Ding), brucebin@bit.edu.cn (B. Xin), chenjie@bit.edu.cn (J. Chen).

https://doi.org/10.1016/j.automatica.2019.108495
0005-1098/

specially practical significance for Dubins vehicles (Yao, Qi, Zhao, & Wan, 2017). Specially, this path prolongation problem is important to achieve coordination among multiple Dubins vehicles. To implement cooperative tasks, multiple vehicles need to reach their targets at the same time or at a certain time interval.

Several methods for elongating the bounded-curvature paths have been reported in the literatures. Bui and Boissonnat (1994) studied the accessibility region which a Dubins vehicle can reach from its initial configuration by following an optimal path whose length is no more than a given value. Schumacher, Chandler, Rasmussen, and Walker (2003) proposed path elongation strategies based on insertion of straight line segments to the original path. Shanmugavel, Tsourdos, Zbikowski, and White (2005) varied the radius of circular arcs to change the length of the path and achieve the simultaneous arrival of multiple unmanned aerial vehicles (UAVs). Meyer, Isaiah, and Shima (2015) provided three strategies to elongate Dubins paths for intercepting a moving target at a given time. Ortiz, Kingston, and Langbort (2013) provided path elongation strategies regarding the path type which is composed of two arcs connected by a straight line. Yao et al. (2017) defined homotopy structures which ensure the monotonicity of path length with respect to homotopy parameters. They searched for Dubins paths with an expected length within the homotopies. In addition, Jeon, Lee, and Tahk (2016), based on optimal control theory, derived a closed form of the Impact Time Control Guidance (ITCG) which can guide a Dubins vehicle to reach a stationary target at a preset time.

It can be seen that the previous works about path elongation mainly focus on how to prolong Dubins path. In this paper, we discuss a fundamental theoretical problem about the path elongatability problem (i.e., the realizability of the curvature-constrained paths for a Dubins vehicle with free terminal heading by any given length). The Dubins path with free terminal heading, proposed by Bui and Boissonnat (1994), refers to a Dubins path whose initial configuration and endpoint are fixed but the terminal heading is free.

The main contribution of this paper is that we prove that a Dubins vehicle with free terminal heading cannot realize the path elongation to an arbitrary length, and there is an unrealizable length interval when the endpoint is located in a special region (see Theorem 6). For all realizable length intervals, an example of feasible path patterns for expected elongation is provided. In addition, we further extend our theoretical results to the case of a Dubins vehicle with variable bounded speed (see Corollary 1).

The remainder of this paper is structured as follows. Mathematical preliminaries and proof outline are given in Section 2. Section 3 and Section 4 discuss the path elongation problem according to different locations of the endpoint. Section 5 summarizes the main results and makes an extension to the case of a Dubins vehicle with bounded speed. Section 6 concludes the paper.

2. Preliminaries and proof outline

2.1. Notation

Denote by γ the path of the Dubins vehicle which follows Eq. (1). The problem proposed in Section 1 can be restated as the following question:

Q1: Suppose that the initial configuration of the Dubins vehicle is $\boldsymbol{\omega_0} = (0, 0, \pi/2)$. Given an endpoint P and a path length d which is larger than the shortest path length d_{min}, can γ go from $\boldsymbol{\omega_0}$ to P satisfying that the length of γ is d?

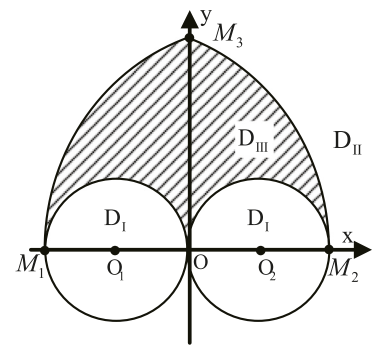

Fig. 1. Division of the entire two-dimensional plane.

Remark 1. Consider that when $\boldsymbol{\omega_0} = (x_0, y_0, \delta)$, $P = (x_P, y_P)$ can be transformed into a coordinate of $P_T = (x_{P_T}, y_{P_T})$ in a new coordinate system where the initial configuration of the Dubins vehicle is $(0, 0, \pi/2)$. Therefore, we set $\boldsymbol{\omega_0} = (0, 0, \pi/2)$. The coordinate transformation can be found in Zeng, Dou, and Xin (2018).

To answer **Q1**, some special circles and corresponding regions are defined in the following. The minimal left-turning circle C_L tangent to the left of y-axis is defined as $C_L = \{(x, y) : (x+r_{\min})^2 + y^2 = r_{\min}^2\}$. Let Ω_L be the closed region bounded by C_L. Analogous interpretations apply for the minimal right-turning circle C_R and Ω_R. The extended left circle C_{EL} has the same center with C_L but a radius of $3r_{\min}$. Let Ω_{EL} be the closed region bounded by C_{EL}. Analogous interpretations apply for the extended right circle C_{ER} and Ω_{ER} for C_R.

The interior and boundary of a set X in a topological space are denoted by $\text{int}(X)$ and $\partial(X)$, respectively. For convenience of discussing **Q1**, the entire two-dimensional plane Ω is divided into three regions which are denoted by D_I, D_{II} and D_{III}, respectively (see Fig. 1). Region D_I is defined as $D_I = \{(x, y) : (x, y) \in \text{int}(\Omega_L \bigcup \Omega_R)\}$. Region D_{II} is defined as $D_{II} = \{(x, y) : (x, y) \in \Omega - \text{int}(\Omega_+ \bigcup \Omega_L \bigcup \Omega_R)\}$, where region Ω_+ is defined as $\Omega_+ = \{(x, y) : (x, y) \in \Omega_{EL} \bigcap \Omega_{ER} \text{ and } y \geq 0\}$. Region D_{III} is defined as $D_{III} = \{(x, y) : (x, y) \in \Omega - D_I \bigcup D_{II}\}$.

2.2. Dubins path

Dubins (1957) found that any Dubins path is composed of a finite set of circle arcs and straight lines. To specify admissible paths, we introduce three elementary path patterns.

- The left-turning arc, denoted by $L^r_{\theta_L}$, means that the Dubins vehicle turns an angle θ_L along its left-turning circle whose radius is r $(r \geq r_{\min})$. In this case, $0 < u \leq 1$.
- The straight line segment, denoted by S, means that the Dubins vehicle moves along a straight line to the endpoint or the starting point of the next path segment. In this case, $u = 0$.
- The right-turning arc, denoted by $R^r_{\theta_R}$, means that the Dubins vehicle turns an angle θ_R along its right-turning circle whose radius is $r(r \geq r_{\min})$. In this case, $-1 \leq u < 0$.

The Dubins path can be represented by combining the elementary path patterns defined above. The length of a Dubins path can be regarded as a function of the path patterns and is denoted by $\mathscr{L}(\cdot)$, e.g., $\mathscr{L}(L^{r_{\min}}_{\theta} R^r\_S)$.

Remark 2. The symbol "−" used in the composite path pattern $L^{r_{\min}}_{\theta} R^r\_S$ and the other descriptions in the sequel implies that, given the other parameters in the path pattern, the turning angle for the corresponding turning arc takes a default value which can be determined uniquely and easily. In this way, it is highlighted that the corresponding angle is not a control parameter for the path pattern.

As the shortest Dubins path is an important reference for path elongation, the following lemma is introduced to expound its possible patterns.

Lemma 1 (Bui & Boissonnat, 1994). *The patterns of the shortest Dubins path with free terminal heading include the following cases:*

- *For $P \in D_I$, the shortest Dubins path is $R_{\theta_L^*}^{r_{\min}} L_-^{r_{\min}}$ ($x_P \le 0$) or $L_{\theta_R^*}^{r_{\min}} R_-^{r_{\min}}$ ($x_P > 0$);*
- *For $P \notin D_I$, the shortest Dubins path is $L_-^{r_{\min}} S$ ($x_P \le 0$) or $R_-^{r_{\min}} S$ ($x_P > 0$).*

Remark 3. In the rest of this paper, we assume that P is in the right-half plane. According to the symmetry implied in the theoretical results, similar conclusions hold for the endpoints in the left-half plane.

2.3. Proof outline

Our main results (Theorem 6) show the realizable path length with respect to P in region D_1, D_{II} and D_{III}, respectively. An interesting and important result is about the path elongatability in the case of $P \in D_{III}$. In this case, two special paths λ^- and β^- are defined (see Propositions 2 and 3). The path length can be adjusted within the interval $[d_{\min}, \mathscr{L}(\lambda^-)] \bigcup [\mathscr{L}(\beta^-), +\infty)$ (see Propositions 1–3). To prove the inrealizability for the length interval $(\mathscr{L}(\lambda^-), \mathscr{L}(\beta^-))$, we skillfully divide all γs from $\boldsymbol{\omega_0}$ to $P \in D_{III}$ into three types: Type I, Type II and Type III. A geometric approach is used to prove that (1) the maximum path length of the Type I paths is $\mathscr{L}(\lambda^-)$ (see Theorem 3); (2) no Type II paths exist (see Theorem 4); and (3) the minimum path length of Type III paths is $\mathscr{L}(\beta^-)$ (see Lemma 3 and Theorem 5). In particular, Corollary 2.4 in Ayala (2017) (see Lemma 2 in this paper) supports the proof by contradiction in Theorem 4. As a result, in the cases of $P \in D_{III}$, there is a length interval $(\mathscr{L}(\lambda^-), \mathscr{L}(\beta^-))$ in which no proper path exists. In the case of $P \in D_I \bigcup D_{II}$, we can use analytical geometry to prove that the Dubins path length can be elongated from $d_{\min}$ to an arbitrary length (see Theorems 1 and 2). In addition, the result of Theorem 6 can be easily extended to the case that v_d is bounded (Corollary 1).

3. Path elongatability in the case of $P \in D_I \bigcup D_{II}$

Considering $D_I \bigcap D_{II} = \varnothing$, results regarding **Q1** are proved with respect to the cases $P \in D_I$ and $P \in D_{II}$ in the following two theorems, respectively.

Theorem 1. *Given $\boldsymbol{\omega_0}$ and $P \in D_I$, the Dubins path length can be elongated from $d_{\min}$ to an arbitrary length.*

Proof. The shortest Dubins path can be described as $L_{\theta_L^*}^{r_{\min}} R_-^{r_{\min}}$ when $P \in \Omega_L$ by Lemma 1, as shown in Fig. 2. When $d > d_{\min}$, the path pattern $L_{\theta_L}^{r_{\min}} R_-^{r_{\min}} S$ can be used to elongate paths by adjusting θ_L ($\theta_L \ge \theta_L^*$). It can be proved that the increase of θ_L will generate a continuous elongation of the shortest path. Let the maximum value of θ_L be π and the path length with respect to $\theta_L = \pi$ is denoted by $d_I = \mathscr{L}(L_\pi^{r_{\min}} R_-^{r_{\min}} S)$.

When $d > d_I$, the path can be further elongated, relative to $L_\pi^{r_{\min}} R_-^{r_{\min}} S$, by increasing the right-turning radius r, as shown in

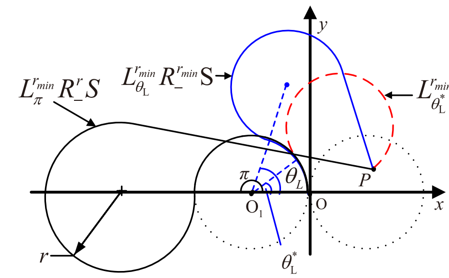

Fig. 2. Path elongation strategies using the path pattern $L_{\theta_L}^{r_{\min}} R_-^{r_{\min}} S$ and $L_\pi^{r_{\min}} R_-^r S$ for $P \in D_I$, respectively.

Fig. 2. The resulting path pattern can be described as $L_\pi^{r_{\min}} R_-^r S$. It is easy to prove that $\mathscr{L}(L_\pi^{r_{\min}} R_-^r S)$ monotonously increases with r, and $\mathscr{L}(L_\pi^{r_{\min}} R_-^r S) \to \infty$ when $r \to \infty$. □

Theorem 2. *Given $\boldsymbol{\omega_0}$ and $P \in D_{II}$, the Dubins path can be elongated to an arbitrary length with the path pattern $L_{\theta_L}^{r_{\min}} R_-^{r_{\min}} S$ for $d_{\min} \le d \le d_I$ by varying θ_L and with the path pattern $L_\pi^{r_{\min}} R_-^r S$ for $d > d_I$ by varying r.*

Proof. Since the analytic formulas of the path length of $L_{\theta_L}^{r_{\min}} R_-^{r_{\min}} S$ and $L_\pi^{r_{\min}} R_-^r S$ are the same as these in Theorem 1, this theorem can be regarded as a direct extension of Theorem 1. In addition, when $P \in D_{II}$, the pattern of the shortest Dubins path is $R_-^{r_{\min}} S$ (Bui & Boissonnat, 1994). The pattern $R_-^{r_{\min}} S$ can be regarded as a degenerate version of $L_{\theta_L}^{r_{\min}} R_-^{r_{\min}} S$ when $\theta_L = 0$. So the parameter θ_L of the pattern $L_{\theta_L}^{r_{\min}} R_-^{r_{\min}} S$ satisfies $\theta_L \in [0, \pi]$. □

4. Path elongatability in the case of $P \in D_{III}$

Proposition 1 (*Lemma 8 in Meyer et al. (2015)*). *If the Dubins vehicle moves from $\boldsymbol{\omega_0}$ to $P \in D_{III}$, increasing the turning radius r of $R_-^r S$ will generate a continuous elongation of the shortest path. However, the parameter r of $R_-^r S$ has an upper bound r_M which corresponds to a degenerate version of this pattern, represented by $R_-^{r_M}$, including only one circular arc.*

When $P \in D_{III}$, the shortest Dubins path is $R_-^{r_{\min}} S$ according to Lemma 1. According to Proposition 1, the length interval $[d_{\min}, \mathscr{L}(R_-^{r_M})]$ is realizable, so what we are concerned next is the realizability of the interval $(\mathscr{L}(R_-^{r_M}), +\infty)$ for $P \in D_{III}$.

The path pattern $L_{\theta_L}^{r_{\min}} R_-^r$ can be used to achieve further elongation. To facilitate analysis, the x–y coordinate system needs to be transformed into a polar coordinate system whose origin is the center of C_L, denoted by O_1. The angle between $\overrightarrow{O_1P}$ and the positive x-axis is denoted by ξ, and the Euclidean distance between P and O_1 is denoted by ρ, as shown in Fig. 3. The different relationship between θ_L and ξ will lead to different feasible elongation schemes (see Fig. 3). For clarity, the pattern $L_{\theta_L}^{r_{\min}} R_-^r$ will be briefly denoted as $L_-^{r_{\min}} R_-^r$ to highlight that r is the unique parameter for the path pattern. Note that, once the parameter r is determined for a given path length, the value of θ_L can be determined uniquely. The following two propositions will discuss the path elongatability with respect to the two cases $\theta_L \le \xi$ and $\theta_L > \xi$, respectively.

Proposition 2. *For a given initial configuration $\boldsymbol{\omega_0}$ and an endpoint $P \in D_{III}$, in the case of $\theta_L \le \xi$, increasing the parameter r in the path pattern $L_-^{r_{\min}} R_-^r$ will generate a limited elongation from $\mathscr{L}(R_-^{r_M})$ to $\mathscr{L}(L_{\theta_L}^{r_{\min}} R_-^{r_{\min}})$. Denote the path $L_{\theta_L}^{r_{\min}} R_-^{r_{\min}}$ by a concise symbol λ^-*

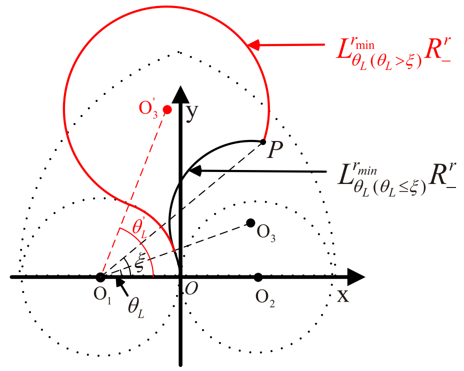

Fig. 3. Path elongation strategies using the path pattern $L_-^{r_{\min}}R_-^r$ for $P \in D_{III}$. The black and red solid curves represent elongated paths by changing r in the case of $\theta_L \le \xi$ and $\theta_L > \xi$, respectively.

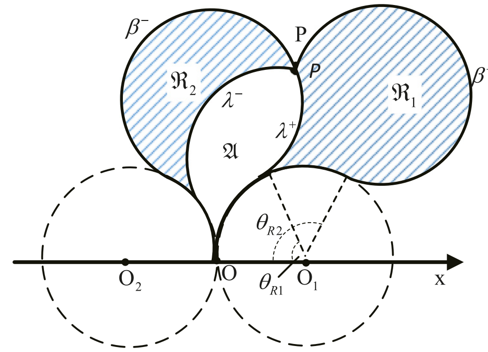

Fig. 4. Regions $\Re_1$, $\Re_2$ and $\mathfrak{A}$.

and its length is

$$\mathscr{L}(\lambda^-) = r_{min}\left[\xi - \arccos\left(\frac{\rho^2 + 3r_{min}^2}{4\rho r_{min}}\right) + \arccos\left(\frac{5r_{min}^2 - \rho^2}{4r_{min}^2}\right)\right]. \tag{2}$$

Proposition 3. *For a given initial configuration $\boldsymbol{\omega_0}$ and an endpoint $P \in D_{III}$, in the case of $\theta_L > \xi$, $\mathscr{L}(L_-^{r_{\min}}R_-^r)$ monotonically increases with r and $\lim_{r\to\infty}\mathscr{L}(L_-^{r_{\min}}R_-^r) = \infty$. $\mathscr{L}(L_-^{r_{\min}}R_-^r)$ will reach its minimum value when $r = r_{\min}$. Denote the path $L_-^{r_{\min}}R_-^{r_{\min}}$ by a concise symbol β^- and its length is*

$$\mathscr{L}(\beta^-) = r_{min}\left[\xi + \arccos\left(\frac{\rho^2 + 3r_{min}^2}{4\rho r_{min}}\right) + 2\pi - \arccos\left(\frac{5r_{min}^2 - \rho^2}{4r_{min}^2}\right)\right]. \tag{3}$$

Propositions 2 and 3 can be easily proved by analyzing the monotonicity of $\mathscr{L}(L_-^{r_{\min}}R_-^r)$ with r in the case of $\theta_L > \xi$ and $\theta_L \le \xi$, respectively. By Propositions 1–3, the realizable length interval of the pattern $\mathscr{L}(L_-^{r_{\min}}R_-^r)$ is $[d_{\min}, \mathscr{L}(\lambda^-)] \bigcup [\mathscr{L}(\beta^-), +\infty)$. Therefore, when $P \in D_{III}$, the path length can be adjusted within the interval $[d_{\min}, \mathscr{L}(\lambda^-)]$ and $[\mathscr{L}(\beta^-), +\infty)$. It can be verified that $\mathscr{L}(\lambda^-) < \mathscr{L}(\beta^-)$ for $P \in D_{III}(x_p \ge 0)$. Now, we are especially interested in the following question:

***Q2**: Can a bounded-curvature path γ go from $\boldsymbol{\omega_0}$ to reach an endpoint in D_{III} with $d \in (\mathscr{L}(\lambda^-), \mathscr{L}(\beta^-))$?*

Definition 1 (*Another Definition for Dubins Path in Dubins (1957)*). Given an initial configuration $\boldsymbol{\omega_0}$ and an endpoint $P = (x_P, y_P)$, a path $\gamma : [0, s] \to \mathbb{R}^2$ connecting $\boldsymbol{\omega_0}$ and P is a bounded-curvature path if:

- γ is C^1 and piecewise C^2 where C^1 stands for a continuous function that has continuous first derivatives and piecewise C^2 stands for a continuous function that has piecewise continuous second derivatives.
- γ is parameterized by arc length s.
- $\gamma(0) = (0, 0)$; $\gamma(s) = (x_P, y_P)$.
- The curvature $\|\gamma''(t)\| \le 1/r_{\min}$, for all $t \in [0, s]$ when defined.

Definition 2 (Ayala, 2017). Given an area Ω, a path $\gamma : [0, s] \to \mathbb{R}^2$ is **in** Ω if $\gamma(t) \subset \Omega$ for all $t \in [0, s]$. Otherwise, γ is **not in** area Ω.

Definition 3 (Ayala, 2017). Given a point $P \in \mathbb{R}^2$ and a maximum curvature $k_{max} = 1/r_{\min}$, the space of the bounded-curvature paths which go from $\boldsymbol{\omega_0}$ and end at P is denoted by $\Sigma(O, P)$.

In the case of $P \in D_{III}$, there are two circles with radius $r = r_{\min}$ which pass through P and are tangent to C_L. Correspondingly, there exist two paths from $\boldsymbol{\omega_0}$ to P whose path pattern is $R_{\theta_R}^{r_{\min}}L_-^{r_{\min}}$. One path $R_{\theta_{R1}}^{r_{\min}}L_-^{r_{\min}}$ is denoted by λ^+, and the other path $R_{\theta_{R2}}^{r_{\min}}L_-^{r_{\min}}$ is denoted by β^+, where $\theta_{R1} \le \theta_{R2}$ (see Fig. 4).

We use $\mathfrak{A}$ to denote the closed region bounded by curve λ^+ and curve λ^-, using $\Re_1$ to denote the closed region bounded by curve λ^+ and curve β^+, and using $\Re_2$ to denote the closed region bounded by curve λ^- and curve β^-, as shown in Fig. 4. To answer **Q2**, all bounded-curvature paths γ with $\gamma \in \Sigma(O, P)$ are divided into three types:

- Type I: γ **in** $\mathfrak{A}$;
- Type II: γ **in** $\mathfrak{A} \bigcup \text{int}(\Re_1 \bigcup \Re_2)$ but **not in** $\mathfrak{A}$;
- Type III: γ **not in** $\mathfrak{A} \bigcup \text{int}(\Re_1 \bigcup \Re_2)$.

Denote the sets of Type I, Type II and Type III paths by Γ_I, Γ_{II} and Γ_{III}, respectively. We conjecture that when $P \in D_{III}$, there is no path $\gamma \in \Sigma(O, P)$ with its path length $d \in (\mathscr{L}(\lambda^-), \mathscr{L}(\beta^-))$. To verify this conjecture, the proof will be demonstrated in the following steps:

(1) Prove that the maximum path length of $\gamma \in \Gamma_I$ is $\mathscr{L}(\lambda^-)$. (See Section 4.1)
(2) Prove that $\Gamma_{II} = \varnothing$. (See Section 4.2)
(3) Prove that the minimum path length of $\gamma \in \Gamma_{III}$ is $\mathscr{L}(\beta^-)$. (See Section 4.3)

4.1. The maximum path length of Type I paths

To find the maximum length for Type I paths, we are inspired by the proof strategy in Howard and Treibergs (1995) to prove that γ and λ^- have a common perpendicular at first, and then prove $\mathscr{L}(\gamma) \le \mathscr{L}(\lambda^-)$.

Theorem 3. *The maximum length of bounded-curvature paths γ in $\mathfrak{A}$ with $\gamma \in \Sigma(O, P)$ is $\mathscr{L}(\lambda^-)$.*

The proof is postponed to Appendix A.

4.2. Inexistence of Type II paths

Lemma 2 (*Corollary 2.4 in Ayala (2017)*). *Suppose a bounded-curvature curve $\gamma : [0, s] \to \mathbb{R}^2$ (its maximum curvature $k_{max} = 1/r_{\min}$) satisfies:*

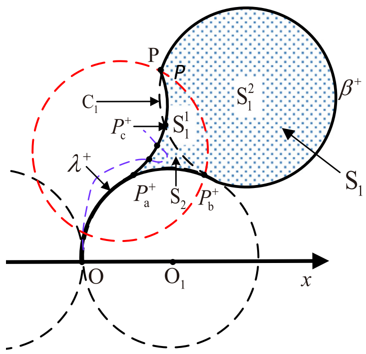

Fig. 5. The bounded-curvature plane curves in $\mathfrak{A}\bigcup\mathrm{int}(S_1)$ and $\mathfrak{A}\bigcup\mathrm{int}(S_2)$, respectively.

(1) $\gamma(0)$, $\gamma(s)$ are points on the x-axis.

(2) If C_M is a circle with center on the negative y-axis and its radius is $r_{\min}$, and $\gamma(0),\gamma(s)\in C_M$, then some point of γ lies above C_M.

Then there is a line joining two points in γ, which are at least $2r_{\min}$ apart.

Theorem 4. *Any bounded-curvature curve $\gamma:(0,s)\to\mathbb{R}^2$ with $\gamma\in\Sigma(O,P)$ which is in $\mathfrak{A}\bigcup\mathrm{int}(\Re_1)$ but not in $\mathfrak{A}$ does not exist.*

Proof. Denote by P_b^+ the joint point of the arc segments $R_{\theta_{R2}}^{r_{\min}}$ and $L_{-}^{r_{\min}}$ of β^+ (see Fig. 5). Denote by C_1 the circle which is extended from the arc $L_{-}^{r_{\min}}$ of β^+. As shown in Fig. 5, C_1 will intersect λ^+ and $R_{\theta_{R2}}^{r_{\min}}$ at P_c^+ and P_b^+, respectively. The arc $\widehat{P_c^+P_b^+}$ divides the region $\mathrm{int}(\Re_1)$ into two subregions which are denoted by S_1 and S_2, respectively. We add an auxiliary arc in S_1 to connect P and P_b^+, and its curvature is $1/r_{\min}$, and the arc divides S_1 into two regions S_1^1 and S_1^2.

The proof is by contradiction. Supposing that there exists a curve γ which is in $\mathfrak{A}\bigcup\mathrm{int}(\Re_1)$ but not in $\mathfrak{A}$, we define a bounded-curvature curve $\sigma\subset\gamma\bigcap\mathrm{int}(\Re_1)$, that is, σ is the part of γ in $\Re_1$. It can be verified that σ satisfies the two conditions in Lemma 2 if σ is only in S_1, S_2 or $S_2\bigcup S_1^2$. However, for any line joining two points X, Y in σ, the distance between X and Y satisfies $|x–y|<2r_{\min}$. The contradiction indicates that σ does not exist.

Suppose that σ passes through S_2, S_1^1 and S_1^2. We define a bounded-curvature curve $\sigma_1\subset\sigma\bigcap S_1^2$. It can be verified that σ_1 satisfies the two conditions in Lemma 2 and $|x–y|<2r_{\min}$ for any line joining the two points X,Y in σ_1. So σ_1 does not exist in this case, either. □

In the same way, we can easily derive that any bounded-curvature curve $\gamma:(0,s)\to\mathbb{R}^2$ with $\gamma\in\Sigma(O,P)$ which is in $\mathfrak{A}\bigcup\mathrm{int}(\Re_2)$ but not in $\mathfrak{A}$ does not exist. Therefore, Type II paths do not exist, that is, $\Gamma_{II}=\varnothing$.

4.3. The minimum path length of Type III paths

Type III paths are the bounded curvature paths γ with $\gamma\in\Sigma(O,P)$ which are not in $\mathfrak{A}\bigcup\mathrm{int}(\Re_1\bigcup\Re_2)$, implying that $\exists P_m\in\gamma:P_m\notin\mathfrak{A}\bigcup\mathrm{int}(\Re_1\bigcup\Re_2)$, equivalently, $\exists P_m\in\gamma:P_m\in\Omega-\mathfrak{A}\bigcup\mathrm{int}(\Re_1\bigcup\Re_2)$.

Denote by C_2 the circle which is extended from β_2^-. Denote by P_b^- the intersection point of the two arc segments of β^-, as shown in Fig. 7. Similarly, define P_b^+, P_a^- and P_a^+ for β^+, λ^- and λ^+, respectively. Define the set $S_0=\mathfrak{A}\bigcup\mathrm{int}(\Re_1\bigcup\Re_2)\bigcup\widehat{P_a^+P_b^+}\bigcup\widehat{P_a^-P_b^-}$.

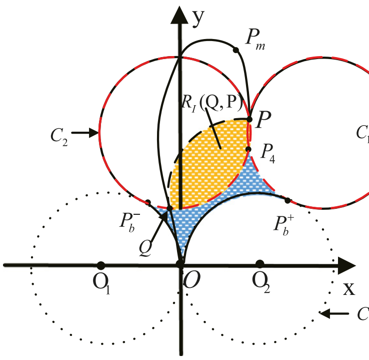

Fig. 6. An illustration of Type III path when $C_2\bigcap C_R=\varnothing$. (For interpretation of the references to color in this figure legend, the reader is referred to the web version of this article.)

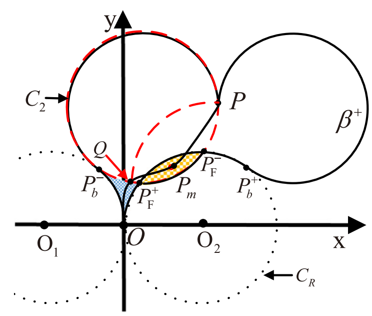

Fig. 7. An illustration of Type III path when $C_2\bigcap C_R\neq\varnothing$. (For interpretation of the references to color in this figure legend, the reader is referred to the web version of this article.)

In the case of $C_2\bigcap C_R\neq\varnothing$, define $C_2\bigcap C_R=\{P_F^+,P_F^-\}$ with $\angle P_F^+O_2O\le\angle P_F^-O_2O$. Before γ finally reaches the endpoint P, γ must pass through the closed area surrounded by the three arcs $\widehat{OP_b^-}$, $\widehat{OP_F^+}$ and $\widehat{P_b^-P_F^+}$ (see the blue shadow area in Fig. 7). Due to the constraint of the maximum curvature, γ needs to pass through $\widehat{P_b^-P_F^+}$. The first point of γ across $\widehat{P_b^-P_F^+}$ is denoted by Q. Obviously, $\gamma_Q\subset S_0$.

In the case of $C_2\bigcap C_R=\varnothing$, define $C_1\bigcap C_2=\{P_3,P_4\}$ with $P_3=(x_3,y_3)$, $P_4=(x_4,y_4)$ and $y_3\ge y_4$. Before γ finally reaches the endpoint P, γ must pass through the closed area surrounded by the four arcs $\widehat{OP_b^-}$, $\widehat{OP_b^+}$, $\widehat{P_b^+P_4}$ and $\widehat{P_b^-P_4}$ (see the blue shadow area in Fig. 6). Due to the constraint of the maximum curvature, γ needs to pass through $\widehat{P_b^-P_4}$ or $\widehat{P_b^+P_4}$ to arrive at P. The first point of γ across $\widehat{P_b^-P_4}$ or $\widehat{P_b^+P_4}$ is denoted by Q. Denote by γ_Q the part of γ from $\boldsymbol{\omega_0}$ to Q and denote by γ_P the part of γ from Q to P. Obviously $\gamma_Q\subset S_0$. The intersection region of the two disks with radius $r_{\min}$ joining P and Q is denoted by $R_I(P,Q)$. Similarly, $R_I(P_F^+,P_F^-)$ is defined.

Before discussing the minimum length for Type III paths, we introduce the following Lemma.

Lemma 3. *Given $\gamma\in\Gamma_{III}$ and an endpoint $P\in D_{III}$, if γ_P is not in $R_I(Q,P)$, then $\mathscr{L}(\gamma)\ge\mathscr{L}(\beta^-)$ holds.*

The proof of this lemma is postponed to Appendix B. The following theorem discusses the minimum length for Type III paths.

Theorem 5. $\mathscr{L}(\gamma)\ge\mathscr{L}(\beta^-)$, $\forall\gamma\in\Gamma_{III}$.

Table 1
An example of path elongation schemes when the endpoint is located in the right-half plane.

Region	Length interval	Typical path pattern	Adjustable parameters
D_I	$[d_{\min}, d_I)$	$L_{\theta_L}^{r_{\min}} R_{-}^{r_{\min}} S$	$\theta_L \in [\theta_L^*, \pi)$
	$[d_I, +\infty)$	$L_{\pi}^{r_{\min}} R_{-}^{r} S$	$r \in [r_{\min}, +\infty)$
D_{II}	$[d_{\min}, d_I)$	$L_{\theta_L}^{r_{\min}} R_{-}^{r_{\min}} S$	$\theta_L \in [0, \pi)$
	$[d_I, +\infty)$	$L_{\pi}^{r_{\min}} R_{-}^{r} S$	$r \in [r_{\min}, +\infty)$
D_{III}	$[d_{\min}, \mathscr{L}(R_{-}^{r_M})]$	$R_{-}^{r} S$	$r \in [r_{\min}, r_M]$
	$(\mathscr{L}(R_{-}^{r_M}), \mathscr{L}(\lambda^-)]$	$L_{-}^{r_{\min}} R_{-}^{r}$	$r \in (r_{\min}, r_M]$
	$(\mathscr{L}(\lambda^-), \mathscr{L}(\beta^-))$	**Unrealizable**	**not available**
	$[\mathscr{L}(\beta^-), +\infty)$	$L_{-}^{r_{\min}} R_{-}^{r}$	$r \in [r_{\min}, +\infty)$

Proof. To find the minimum path length for Type III paths, two cases are discussed as follows:

Case 1 ($C_2 \bigcap C_R \neq \varnothing$). When γ_P is not in $R_I(Q, P)$, Lemma 3 implies that $\mathscr{L}(\gamma) \geq \mathscr{L}(\beta^-)$. However, when γ_P is in $R_I(Q, P)$, $\gamma_P \subset R_I(Q, P)$. Define $S_F = R_I(P_F^+, P_F^-) - C_R$ (the region S_F is shown as the orange shadow area in Fig. 7), such that $S_F \bigcap S_0 = \varnothing$. Since $\gamma_Q \subset S_0$ and $\gamma \bigcap (\Omega - S_0) \neq \varnothing$, $\exists P_m \in \gamma_P$: $P_m \in S_F$. It can be verified that the shortest Dubins path from $\boldsymbol{\omega_0}$ to P_m is no less than $\mathscr{L}(\beta^-)$ by their geometrical relationship. Therefore, $\mathscr{L}(\gamma) \geq \mathscr{L}(\beta^-)$.

Case 2 ($C_2 \bigcap C_R = \varnothing$). Obviously $R_I(Q, P) \subset S_0$. Since $\gamma \bigcap (\Omega - S_0) \neq \varnothing$ and $\gamma_Q \subset S_0$, $\gamma_P \bigcap (\Omega - S_0) \neq \varnothing$. It implies $\gamma_P \bigcap (\Omega - R_I(Q, P)) \neq \varnothing$, that is, γ_P is not in $R_I(Q, P)$, as shown in Fig. 6. Lemma 3 implies $\mathscr{L}(\gamma) \geq \mathscr{L}(\beta^-)$.

If $P_4 = P = Q$, then $R_I(Q, P) = \varnothing$. The shortest length for a closed bounded-curvature curve from Q to Q is $2\pi r_{\min}$ (Theorem 4.14 in Ayala (2017)). Therefore, $\mathscr{L}(\gamma) \geq 2\pi r_{\min} + \gamma_Q^* \geq \mathscr{L}(\beta^-)$, where γ_Q^* is the shortest Dubins path from $\boldsymbol{\omega_0}$ to Q. □

5. Summary and extension

5.1. Main results

According to the discussions in Sections 3 and 4, the main results in this paper are summarized as follows:

Theorem 6. *Given $\boldsymbol{\omega_0}$ and $P \in \mathbb{R}^2$, if $P \in D_{III}$, then there is a length interval $(\mathscr{L}(\lambda^-), \mathscr{L}(\beta^-))$ for which no proper Dubins path exists; otherwise, the Dubins path can be elongated by an arbitrary expected length.*

Proof. Since $D_I \bigcup D_{II} = \Omega - D_{III}$, the Dubins path can be elongated by an arbitrary expected path length if $P \in \Omega - D_{III}$ by Theorems 1 and 2. If $P \in D_{III}$, by applying Theorems 3–5, it can be concluded that there is a length interval $(\mathscr{L}(\lambda^-), \mathscr{L}(\beta^-))$ for which no proper Dubins path exists. □

According to the classification of situations with regard to the location of endpoints and the interval of expected path lengths, a typical example of feasible path patterns for expected elongation is presented in Table 1 when P is located in the right-half plane. In view of the symmetry of the results, through exchanging the pattern notations L and R as shown in Table 1, the conclusions can be easily obtained when P is located in the left-half plane. In addition, in the case of $P \in D_{III}$, different P may lead to different interval lengths for the normalized inrealizable interval $(\mathscr{L}(\lambda^-), \mathscr{L}(\beta^-))$. Fig. 8 shows the normalized interval length $\Delta = (\mathscr{L}(\beta^-) - \mathscr{L}(\lambda^-))/r_{\min}$ as a function of $P/r_{\min}$.

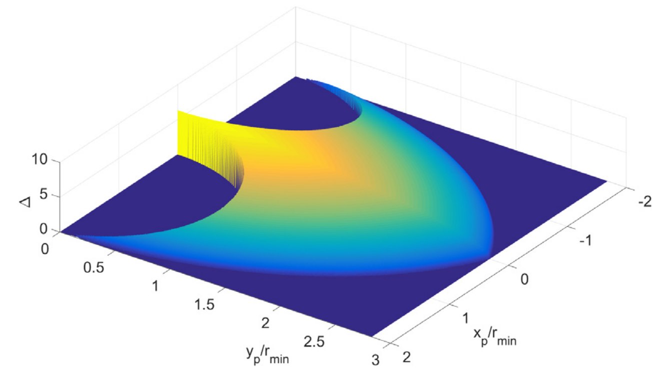

Fig. 8. Normalized length of inrealizable interval Δ as a function of normalized position $P/r_{\min}$.

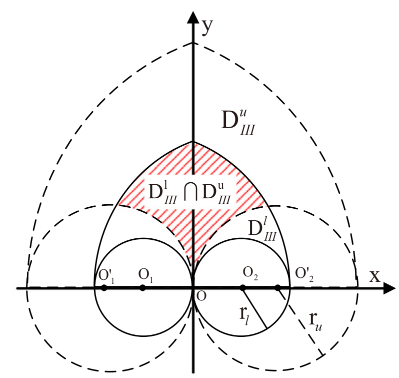

Fig. 9. Region of the endpoint for which there is an unrealizable length interval in the case of bounded variable speed.

5.2. Extended results about bounded variable speed

Generally, the speed v_d is constant in the model of Dubins vehicle. However, our results can easily be extended to the case that v_d is bounded ($v_d \in [v_l, v_u]$ and $0 < v_l \leq v_u$). When v_d reaches its upper bound v_u, $r_{\min}$ will reach its maximum (denoted by r_u) since $r_{\min}$ is proportional to v_d. In this case, new D_{III}, λ^- and β^- under $r_{\min} = r_u$ can be obtained and denoted by D_{III}^u, λ_u^- and β_u^-, respectively. Theorem 6 implies that there is an unreachable length interval $(\mathscr{L}(\lambda_u^-), \mathscr{L}(\beta_u^-))$ if $P \in D_{III}^u$. In the same way, when $v_d = v_l$, $r_{\min}$ will reach its minimum (denoted by r_l). In this case, new D_{III}, λ^- and β^- under $r_{\min} = r_l$ can be denoted by D_{III}^l, λ_l^- and β_l^-, respectively. According to Theorem 6, there is also an unreachable length interval $(\mathscr{L}(\lambda_l^-), \mathscr{L}(\beta_l^-))$ if $P \in D_{III}^l$.

Since $D_{III}^l \bigcap D_{III}^u \neq \varnothing$ (see Fig. 9), there is an unrealizable length interval for which no proper path exists if $P \in D_{III}^l \bigcap D_{III}^u$. According to the monotonicity of $\mathscr{L}(\lambda^-)$ and $\mathscr{L}(\beta^-)$ with respect to $r_{\min}$ ($r_{\min} \in [r_l, r_u]$), it can be obtained that $\mathscr{L}(\lambda_l^-) > \mathscr{L}(\lambda_u^-)$ and $\mathscr{L}(\beta_l^-) < \mathscr{L}(\beta_u^-)$. Thus, the unrealizable length interval is $(\mathscr{L}(\lambda_l^-), \mathscr{L}(\beta_l^-))$. Therefore, we obtain the following corollary.

Corollary 1. *Given $\boldsymbol{\omega_0}$ and $P \in \mathbb{R}^2$, for $v_d \in [v_l, v_u]$, if $P \in D_{III}^l \bigcap D_{III}^u$, then there is a length interval $(\mathscr{L}(\lambda_l^-), \mathscr{L}(\beta_l^-))$ for which no proper Dubins path exists. Otherwise, the Dubins path can be elongated by an arbitrary expected path length.*

5.3. Simulation

We present two simulation examples to demonstrate the path elongation of a UAV modeled by Eq. (1) in the case of $P \in D_{III}$

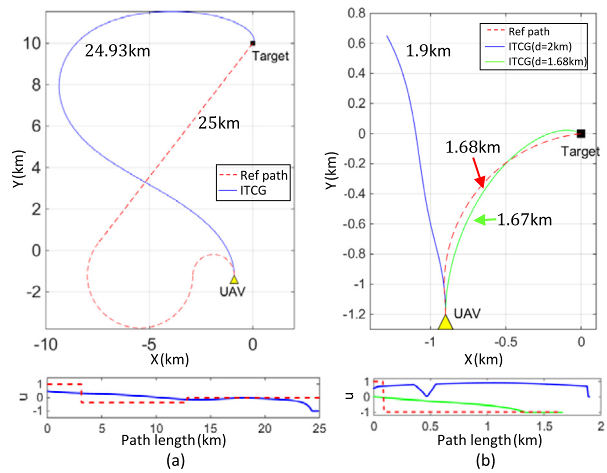

Fig. 10. Reference paths as well as trajectories generated by ITCG and their control input u with respect to path length. (a) $P = (0, 10)$ km, and (b) $P = (0, 0)$ km . (For interpretation of the references to color in this figure legend, the reader is referred to the web version of this article.)

and $P \notin D_{III}$. In the two examples, reference paths are generated by the path elongation scheme presented in Table 1. The UAV can stably follow the reference paths by a path following method (e.g., Balluchi, Bicchi, and Souères (2005)). We also provide the elongated paths generated by ITCG, proposed by Jeon et al. (2016), which can drive UAV to reach the target at a given time.[1]

The UAV is initially at $\boldsymbol{\omega_0} = (-0.9 \text{ km}, -1.2 \text{ km}, \pi/2)$ and $r_{min} = 1$ km. In the first example, we set an endpoint $P = (0, 10)$ km and the desired length $d = 25$ km. It can be verified that P is located in D_{II} for the UAV with respect to $\boldsymbol{\omega_0}$, so the elongated paths exist according to Theorem 2. The reference path with path pattern $L_{\pi}^{r_{\min}} R^{r}\_S$ and the trajectory generated by ITCG can be obtained (see the red and blue curves in Fig. 10(a), respectively).

In the second example, we set $P = (0, 0)$ km and $d = 2$ km. It can be verified that P is located in D_{III} for the UAV with respect to $\boldsymbol{\omega_0}$ and $d \in (\mathscr{L}(\lambda^-), \mathscr{L}(\beta^-)) = (1.68, 5.73)$ km, so UAV cannot realize path elongation according to Theorem 6. If we implement ITCG in this case, it can be observed that the UAV cannot arrive at the target with d (see the blue curve in Fig. 10(b)), which is consistent with the theoretical results presented in Theorem 6. If d is reset as $\mathscr{L}(\lambda^-) = 1.68$ km, Proposition 2 implies that the elongated paths exist. The reference path with path pattern $L\_^{r_{\min}} R\_^{r}$ and the path generated by ITCG can be obtained (see the red and green curves in Fig. 10(b), respectively).

6. Conclusion

In this paper, we study the path elongation problem of a Dubins vehicle from a given configuration to any destination point in the two-dimensional plane. As the main contribution of the paper, we discover and prove that, when the destination point is located in D_{III}, there is a length interval for which no proper path exists. For all realizable length intervals, we provide an example of feasible path patterns for expected elongation. The theoretical results obtained in this paper can be referenced to adjust the path of a curvature-constrained vehicle to achieve the time control for the vehicle to reach a given destination.

In future work, more feasible path patterns and elongation schemes for expected elongation will be investigated. Besides, in practice, there are some applications which may need to constrain the terminal heading (e.g., exploration or inspections in which a camera or other sensor has to be pointed in a specific orientation). In the future, the path elongation problem with terminal heading constraint will be investigated.

[1] Note that the aim of presenting the results of ITCG is to demonstrate the realizability of the Dubins paths with given lengths instead of comparison.

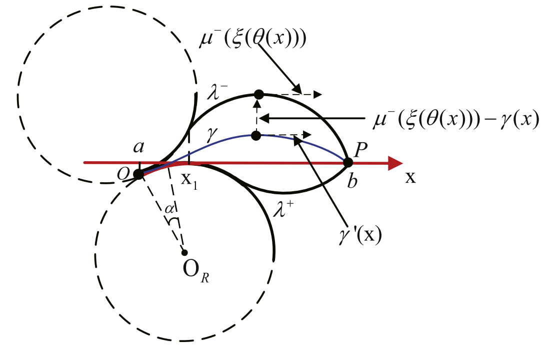

Fig. A.1. A common perpendicular with γ and λ^-.

Appendix A. Proof of Theorem 3

The heading angle for the bounded-curvature path γ with $\gamma \in \Sigma(O, P)$ is denoted by $\theta(s)$. $\theta(s) = \int_0^s k(t)\mathrm{d}t + \frac{\pi}{2}$. The x-coordinate of γ is denoted by $x(s)$. According to the nonholonomic constraint of the Dubins vehicle model, $\mathrm{d}x/\mathrm{d}s = \cos\theta$, such that $x(s) = \int_0^s \cos(\theta(s))\mathrm{d}t$. The shortest path from $\boldsymbol{\omega_0}$ to P is denoted by λ and the length of its arc segment is denoted by α. By a rotation, we may assume that $\lambda(\alpha)$ is the coordinate origin and the tangent vector $\lambda'(\alpha)$ defines the positive x-axis. Let a and b ($a < b$) be the x-coordinates of O and P, respectively, as shown in Fig. A.1. $\gamma'(s) = \exp(i\theta(s))$, and similarly $(\lambda^-)'(s) = \exp(i\theta^-(s))$. Let x_1 ($a < x_1 < b$) be the x-coordinate of the endpoint of the first arc segment of λ^-, as shown in Fig. A.1. According to the result in Howard and Treibergs (1995) (see eq. (4.2) therein), we have

$$
\begin{aligned}
&\frac{\mathrm{d}\theta}{\mathrm{d}x} = \frac{\mathrm{d}\theta}{\mathrm{d}s}\frac{\mathrm{d}s}{\mathrm{d}x} = k(s)\sec\theta, \quad |k(s)| \le 1 \\
&\frac{\mathrm{d}\theta^-}{\mathrm{d}x} = \frac{d\theta^-}{\mathrm{d}s^-}\frac{\mathrm{d}s^-}{\mathrm{d}x} = \begin{cases} +\sec\theta^-, & \text{if } a < x < x_1 \\ -\sec\theta^-, & \text{if } x_1 < x < b. \end{cases}
\end{aligned}
\tag{A.1}
$$

Since $\theta(0) = \theta^-(0)$, the comparison theorem for (A.1) implies $\theta(x_1) \le \theta^-(x_1)$. Denote the second arc segment of λ^- by μ^-. For each $\zeta \in [\theta^-(x_1), \theta^-(b)]$, there is a unique x-coordinate $\nu(\zeta)$ where the heading angle of μ^- is ζ. Consider the continuous inner product function

$$f(x) = \langle \gamma'(x), \mu^-(\nu(\theta(x))) - \gamma(x) \rangle$$

to measure the distance between the normal lines thru $\gamma(x)$ and μ^- at points with parallel tangents, as shown in Fig. A.1. Observe that $f(x_1) \ge 0$ and $f(b) \le 0$. By the intermediate value theorem, there is an $x_2 \in [x_1, b]$ where the normal lines of γ and μ^- coincide. Hence by a rotation, we may assume that this line is the y-axis and x_2 is the new coordinate origin denoted as O'.

Next we will show that $\mathscr{L}(\lambda^-) \ge \mathscr{L}(\gamma)$. It suffices to compare the lengths of the parts corresponding to $x \ge 0$ and $x \le 0$ separately. Let a ($a \le 0$) and b ($b \ge 0$) again be the ending x-coordinates of γ. Let $x_1 (a < x_1 < b)$ again be the x-coordinate of the endpoint of the first arc segment of λ^-.

Since $\theta(a) = \theta^-(a)$, the equality $\sin(\theta(a)) = \sin(\theta^-(a))$ holds. Thus, from the comparison theorem, Eq. (A.1) implies $\sin(\theta^-(x)) \ge \sin(\theta(x))$ $(\forall x \in (a, x_1))$, which further leads to the inequality $\theta^-(x) \ge \theta(x)$ $(\forall x \in (a, x_1))$. In the same way, it can be obtained that $\theta^-(x) \ge \theta(x)$ ($\forall x \in (x_1, 0]$) and $\theta^-(x) \le \theta(x)$ ($\forall x \in [0, b)$). Hence,

$$\frac{\mathrm{d}s^-}{\mathrm{d}x} = \sec(\theta^-(x)) \ge \sec(\theta(x)) = \frac{\mathrm{d}s}{\mathrm{d}x}, \quad \forall x \in (a, b). \tag{A.2}$$

Since $s^-(a) = s(a) = 0$, Eq. (A.2) implies that $s^-(b) \ge s(b)$, i.e., $\mathscr{L}(\lambda^-) \ge \mathscr{L}(\gamma)$. □

Appendix B. Proof of Lemma 3

In the case of $Q \in C_2$, let $\mathscr{L}(\beta_2^-) = \mathscr{L}(\beta^-) - |\widehat{QP_b^-}|$. It can be easily verified that $\mathscr{L}(\beta_2^-)$ monotonically decreases with ρ, and $\mathscr{L}(\beta_2^-) \to \pi r_{min}$ when $\rho \to 3r_{min}$, such that $\mathscr{L}(\beta_2^-) > \pi r_{min}$, so $|\widehat{PQ}| \le 2\pi r_{min} - \mathscr{L}(\beta_2^-) < \pi r_{min}$. Therefore, the minimal length of γ_P is the length of the longer arc between P and Q (Corollary 4.15 in Ayala (2017)), that is $\widehat{QP_b^- P}$, as shown in Fig. 6. Therefore,

$$\mathscr{L}(\gamma) \ge |\widehat{QP_b^- P}| + \mathscr{L}(\gamma_Q) = \mathscr{L}(\gamma_Q) + |\widehat{QP_b^-}| + \mathscr{L}(\beta_2^-). \tag{B.1}$$

Furthermore, the shortest Dubins path from $\boldsymbol{\omega_0}$ to Q is denoted by γ_Q^*, such that $\mathscr{L}(\gamma_Q) \ge \mathscr{L}(\gamma_Q^*)$. Since β_1^- is a convex arc and $\gamma_Q^* \bigcup \widehat{QP_b^-}$ lies above β_1^-, $\mathscr{L}(\beta_1^-) \le |\widehat{QP_b^-}| + \mathscr{L}(\gamma_Q^*)$ (Proposition 7 in Dubins (1957)). Therefore,

$$\mathscr{L}(\gamma) \ge \mathscr{L}(\gamma_Q^*) + |\widehat{QP_b^-}| + \mathscr{L}(\beta_2^-) \ge \mathscr{L}(\beta_1^-) + \mathscr{L}(\beta_2^-) = \mathscr{L}(\beta^-). \tag{B.2}$$

In a similar way, it can be proved that $\mathscr{L}(\gamma) \ge \mathscr{L}(\beta^+)$ in the case of $Q \in C_1$. Consider that $P \in D_{III}$ is located in the right half-plane, it can be easily verified that $\mathscr{L}(\beta^+) \ge \mathscr{L}(\beta^-)$ according to their analysis formulas. So $\mathscr{L}(\gamma) \ge \mathscr{L}(\beta^-)$. □

References

Ayala, J. (2017). On the topology of the spaces of curvature constrained plane curves. *Advances in Geometry*, *17*(3), 283–292.

Babel, L. (2017). Curvature-constrained traveling salesman tours for aerial surveillance in scenarios with obstacles. *European Journal of Operational Research*, *262*(1), 335–346.

Balluchi, A., Bicchi, A., & Souères, P. (2005). Path-following with a bounded-curvature vehicle: a hybrid control approach. *International Journal of Control*, *78*(15), 1228–1247.

Bui, X., & Boissonnat, J. (1994). Accessibility region for a car that only moves forwards along optimal paths. Technical Report N2181, INRIA, France.

Cao, J., Cao, J., Zeng, Z., & Lian, L. (2016). Optimal path planning of underwater glider in 3D dubins motion with minimal energy consumption. In *Proceeding of OCEANS 2016* (pp. 1–7). Shanghai, China.

Cao, J., Cao, J., Zeng, Z., Yao, B., & Lian, L. (2017). Toward optimal rendezvous of multiple underwater gliders: 3D path planning with combined sawtooth and spiral motion. *Journal of Intelligent and Robotic Systems*, *85*, 1–18.

Dubins, L. E. (1957). On curves of minimal length with a constraint on average curvature, and with prescribed initial and terminal positions and tangents. *American Journal of Mathematics*, *79*(3), 497–516.

Hernàndez, J. D., Moll, M., Vidal, E., Carreras, M., & Kavraki, L. E. (2016). Planning feasible and safe paths online for autonomous underwater vehicles in unknown environments. In *Proceeding of 2016 IEEE/RSJ international conference on intelligent robots and systems (IROS)* (pp. 1313–1320). Daejeon, Korea.

Howard, R., & Treibergs, A. (1995). A reverse isoperimetric inequality, stability and extremal theorems for plane-curves with bounded curvature. *The Rocky Mountain Journal of Mathematics*, *25*(2), 635–681.

Jeon, I. S., Lee, J. I., & Tahk, M. J. (2016). Impact-time-control guidance with generalized proportional navigation based on nonlinear formulation. *Journal of Guidance Control Dynamics*, *39*(8), 1887–1892.

Meyer, Y., Isaiah, P., & Shima, T. (2015). On Dubins paths to intercept a moving target. *Automatica*, *53*, 256–263.

Ortiz, A., Kingston, D., & Langbort, C. (2013). Multi-UAV velocity and trajectory scheduling strategies for target classification by a single human operator. *Journal of Intelligent and Robotic Systems*, *70*, 255–274.

Schumacher, C., Chandler, P. R., Rasmussen, S. J., & Walker, D. (2003). Path elongation for UAV task assignment. In *Proceedings of the AIAA guidance, navigation, and control conference* (pp. 1–10). Austin, United States.

Shanmugavel, M., Tsourdos, A., Zbikowski, R., & White, B. A. (2005). Path planning of multiple UAVs using Dubins sets. In *Proceeding of the AIAA guidance, navigation, and control conference and exhibit* (pp. 15–18). San Francisco, California.

Yao, W., Qi, N., Zhao, J., & Wan, N. (2017). Bounded curvature path planning with expected length for Dubins vehicle entering target manifold. *Robotics and Autonomous Systems*, *97*, 217–229.

Zeng, J., Dou, L., & Xin, B. (2018). A joint mid-course and terminal course cooperative guidance law for multi-missile salvo attack. *Chinese Journal of Aeronautics*, *31*(6), 1311–1326.

Zhang, X., Chen, J., Xin, B., & Peng, Z. (2014). A memetic algorithm for path planning of curvature-constrained UAVs performing surveillance of multiple ground targets. *Chinese Journal of Aeronautics*, *27*(3), 622–633.

Yulong DING received the B.Sc. degree from Qilu University of Technology, Jinan, China, in 2012, and the M.Sc. degree from Xiamen University, Xiamen, China, in 2015. He is currently pursuing the Ph.D. degree with the School of Automation, Beijing Institute of Technology, Beijing. His current research interests include UAV–UGV collaborative systems, heterogeneous multi-agent systems, and task planning of multi-robot systems. Email: dingyvlong@bit.edu.cn.

Bin XIN received the B.Sc. degree in Information Engineering and the Ph.D. degree in Control Science and Engineering, both from the Beijing Institute of Technology, Beijing, China, in 2004 and 2012, respectively. He was an academic visitor at the Decision and Cognitive Sciences Research Centre, the University of Manchester, from 2011 to 2012. He is currently a professor with the School of Automation, Beijing Institute of Technology. His current research interests include search and optimization, evolutionary computation, combinatorial optimization, and multi-agent systems. He is an Associate Editor of the Journal of Advanced Computational Intelligence and Intelligent Informatics and the journal Unmanned Systems. Email: brucebin@bit.edu.cn.

Jie CHEN received the B.Sc., M.Sc., and Ph.D. degrees in Control Theory and Control Engineering from the Beijing Institute of Technology, in 1986, 1996, and 2001, respectively. From 1989 to 1990, he was a visiting scholar in the California State University, U.S.A. From 1996 to 1997, he was a research fellow in the School of E&E, University of Birmingham, U.K. He is currently a professor of control science and engineering, the Beijing Institute of Technology, China. He is also an academician of the Chinese Academy of Engineering. He serves as a managing editor for the Journal of Systems Science and Complexity (2014–2019) and an associate editor for the IEEE Transactions on Cybernetics (2016–2019) and many other international journals. His main research interests include intelligent control and decision in complex systems, multi-agent systems, and optimization methods. He has co-authored 4 books and more than 200 research papers. Email: chenjie@bit.edu.cn.